Flow-Induced Transverse Electrical Potential across an Assembly of Gold Nanoparticles

Chandramouli Subramaniam and T. Pradeep*

Unit on Nanoscience and Technology (UNANST-DST), Department of Chemistry and Sophisticated Analytical Instrument Facility, Indian Institute of Technology Madras, Chennai 600036, India

J. Chakrabarti†

S. N. Bose National Centre for Basic Sciences, Block JD, Sector III, Salt Lake, Kolkata 700091, India

(Received 9 February 2005; published 10 October 2005)

We report the generation of a potential difference, of the order of tens of millivolts, induced by the flow of polar liquids over an assembly of gold nanoparticles. The device consisted of two conducting glass plates, one of which contained the gold nanoparticle multilayer assembly. The potential generated is in transverse direction to the flow and is dependent on the nature of the flowing liquid. We propose a simple theoretical model to account qualitatively for the generation of the flow-induced transverse potential.

DOI: 10.1103/PhysRevLett.95.164501 PACS numbers: 47.60.+i, 47.65.+a, 73.22.−f

Nanoparticles show diverse properties, which make them important in several areas ranging from chemistry to biology. Optical, electrical, and magnetic properties of these materials are being used for novel applications. Here, we report the generation of an electrical potential ~5–30 mV when polar liquids flow over an assembly of metal nanoparticles which illustrates the potentiality of such assemblies as flow sensor devices. The potential, generated in a direction transverse to the flow, is found to increase with the flow rate linearly at large flow rates. It depends on the dipole moment and the ionic concentration of the flowing fluid. The voltage response being transverse to the flow is unlike the earlier reports of flow-induced potential [1–4].

The sensor device consisted of two conducting glass substrates whose conducting surfaces face each other with an insulating spacer of 200 μm thickness. The substrate (indium doped tin oxide conducting glass plate) was cleaned with a mild detergent solution, sonicated with deionized water, and soaked in a 10% solution of HCl for activation. They were then washed with water, dried at 110 °C for 1 h, annealed at 450 °C for 6 h, and cooled in a desiccator. One of the plates was dipped for 2–5 min in a 3% solution of 3-aminopropyl triethoxy silane (anchor molecule) in 2-propanol to create a monolayer of the molecule on the substrate. The plate was removed and heated at 110 °C for 10 min to remove the solvent, cooled, and then dipped in an aqueous solution of 10 nm mean diameter Au@citrate [5] for 10–15 min. The plate was washed with water followed by 2-propanol to remove the unabsorbed species and finally dipped in a 30 m*M* solution of 1,6-hexanedithiol (spacer molecule) in 2-propanol. The spacer molecules help in separating the successive nanoparticle layers. The dipping in Au@citrate and 1,6-hexandithiol were repeated to achieve the desired number of layers (three) [6], shown schematically in the inset of Fig. 1(a). The absorption spectrum of these layers showed a characteristic peak at 520 nm [7] due to the surface plasmon resonance of the parent Au@citrate. Note that both the anchor and spacer molecules are insulators.

We passed the distilled analyte liquid through a cylindrical glass tube of 22 mm inner diameter and 360 mm length, within which the sensor device was suspended as shown in Fig. 1(a). A peristaltic pump regulated the liquid flow against gravity, and care was taken so that no air bubble was trapped within. The potential difference across the plates was measured by a Keithley 2700 multimeter/data acquisition system. In a typical measurement, after stabilization of the liquid flow through the setup (200 s), the electrodes were shorted and subsequently the reading was collected for a period of 4000 s. Then the electrodes were shorted again for a period of 100 s and the measurement was repeated. The plate containing the multilayer assembly was connected to the negative terminal of the voltmeter and a positive reading was obtained, confirming the accumulation of negative charge carriers on this plate. A typical voltage response over many cycles is shown in the inset of Fig. 1(b). Curve *A* in Fig. 1(b) blows up the response of the device over one measurement cycle with water at a flow rate of 500 cm^3/h. The potential difference saturates to 18.3 mV in about 200 s. Experiments done by connecting the voltmeter terminals to the ends of the same plate showed a negligible potential difference (< 1 μV), thereby confirming that the surface of the device is equipotential without any significant longitudinal potential drop, quite unlike the other known cases of flow-induced potential difference [1–4]. The transverse potential drop in curve *A* of Fig. 1(b) can be contrasted to that of curve *B* in the same figure, which shows a negligibly small voltage generated across the plates without the nanoassembly, confirming that the voltage response is due to the nanoparticle layer. The UV-visible spectrum of the multilayer assembly at each stage ascertained that the sample was unaffected by the liquids used during the flow. When the device was suspended in still water, the response was

~1–2 mV, reiterating the fact that the moving liquid was responsible for the potential.

A plot of the saturated value of potential difference, (ϕ_s) versus flow rate is shown in Fig. 1(c). Note that ϕ_s increases with the flow rate and shows a linear dependence at large flow rates [8]. Figure 1(d) shows that ϕ_s decreases as the dipole moment of the flowing liquid increases. All these measurements were conducted for a flow rate of 500 cm^3/h for the liquids, 2-propanol, water, acetone, and acetonitrile with dipole moments of 1.56, 1.85, 2.88, and 3.92 D, respectively. These observations indicate a role of the Coulomb scattering of electrons [9] on the nanoparticle surface by the flowing dipoles. Figure 1(e) further confirms the role of electrical interactions, for ϕ_s decreases as the concentration of trisodium citrate salt increases in the flowing water. Note that Ghosh *et al.* [1] reported the generation of a potential, exponentially dependent on the flow velocity along the flow direction in a carbon nanotube. This is attributed to the scattering of the charge carriers in the nanotube due to the asymmetric ratchet of a fluctuating Coulomb field of the flowing liquid. The asymmetry occurs due to the velocity gradient created at the flowing liquid-nanotube interface. The geometry of our system and the observation of the transverse potential alone rules out this sort of mechanism. Further, the phonon-drag mediated mechanism [3] predicts a potential difference linearly dependent on the flow rate and the viscosity of the flowing fluid, albeit longitudinal to the flow. In order to rule out any such mechanism, we carried out the experiments with fluids of different viscosities obtained by mixing 2-propanol with water. The dependence of ϕ_s on the viscosity of the flowing liquid [Fig. 1(f)] lacks any particular feature and does not comply with the phonon-drag mechanism. A multilayer assembly of gold nanoparticles fabricated on an insulating glass plate, failed to yield any significant transverse and longitudinal potential differences. Hence, the observed potential difference in the case of conducting glass plates is not due to unbalanced electrification of the plates. Moreover, negligible potential differences were observed both in the transverse (< 3 mV) and longitudinal (< 1 μV) directions to the flow when the nanoparticle assembled plate was replaced with a thin (2000 Å) gold film coated plate, ruling out electrokinetic effects [2].

In order to build up the qualitative model, we consider for simplicity a collision between a single dipole of moment μ in the flowing liquid and an electron of charge $-e$ on the surface of a single nanoparticle grafted on a plate. Since the other plate in the experiment is at a large distance compared to the size of the nanoparticle, we take a semi-infinite geometry as shown in Fig. 2(a). The ξ axis is the flow direction parallel to the plate and the z axis normal to

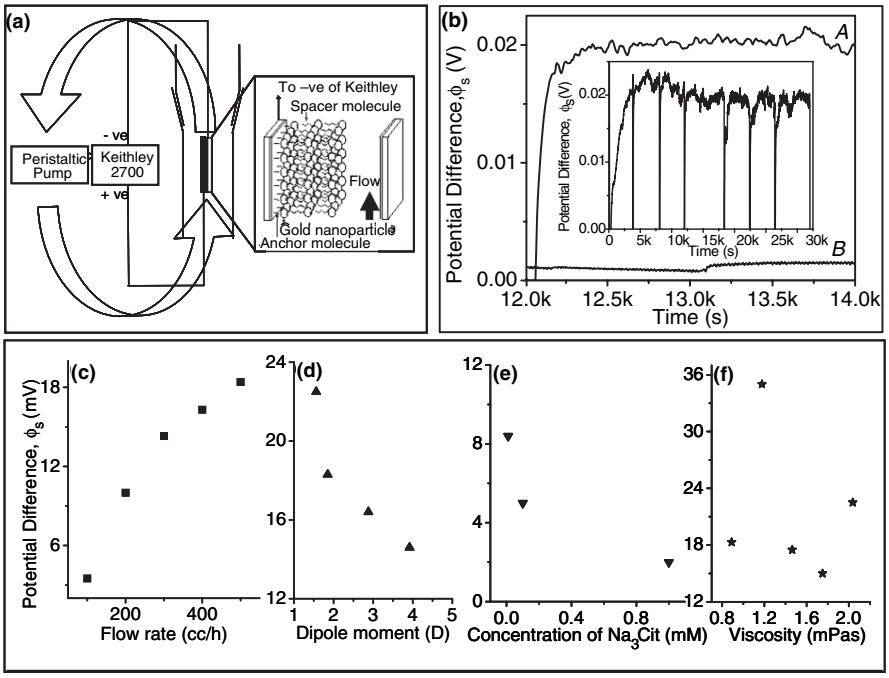

FIG. 1. (a) Schematic of the experimental setup. The cylindrical column housing the device is shown only partly. The device has been blown up (not to scale) on the right showing the nanoparticles, the anchor and the spacer molecules. Estimated thickness of the assembly 100 Å. (b) Plot of the potential difference versus time: *A* Showing the rise and stabilization of the potential difference during 12 000 to 14 000 s (after starting the experiment) *B* for a device without nanoparticles. Inset: Potential difference versus time for a series of measurements, as described in text. Plots of ϕ_s as a function of (c) flow rate, (d) dipole moment, (e) salt concentration (trisodium citrate, Na_3Cit), and (f) viscosity, the flow rate being 500 cm^3/h for (d)–(f).

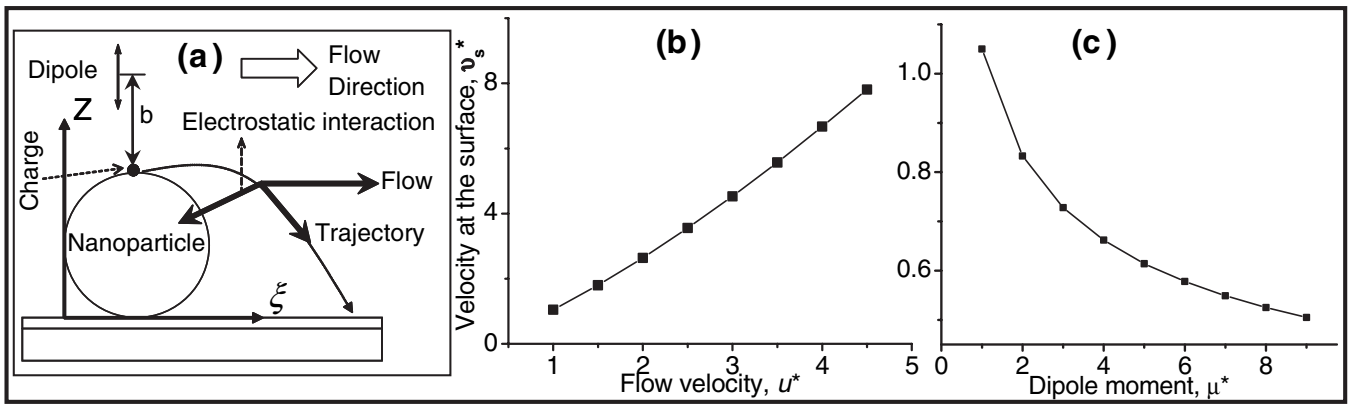

FIG. 2. (a) Schematic representation of the geometry of collision and the subsequent ejection of the electron. The dominant competing forces acting on the ejected charge are indicated. Plot of velocity of the charge at the plate, as a function of (b) flow velocity and (c) dipole moment of the analyte.

the plate, the plate being at $z = 0$. Since the flow velocity, u, is small, we treat the collision nonrelativistically. The motion of the dipole is assumed to remain unchanged during the collision [10]. The impulse experienced by the charge on the nanoparticle due to the electric field, $\vec{E}$ produced by the moving dipole with dipole moment parallel to z axis, would lead to change in momentum of the charge, given by [9] $\delta\vec{p} = -\int_{-\infty}^{+\infty} e\vec{E}dt$, t being the time and the components of $\vec{E}$: $E_Z = [3n_Z(n_Z\mu) - \mu]/[(b^2 + u^2t^2)]^{3/2}$ and $E_\xi = [3n_\xi(n_\xi\mu) - \mu]/[(b^2 + u^2t^2)]^{3/2}$, where $n_Z = b/[(b^2 + u^2t^2)]^{1/2}$ and $n_\xi = ut/[(b^2 + u^2t^2)]^{1/2}$ are the components of the unit vector along the vector connecting the dipole center and the charge, and b the impact parameter, namely, the closest distance of approach between the colliding dipole and the charge [9]. The range of integration over time is taken to be $(-\infty, +\infty)$ due to the slow falling of the coulomb interaction. Note that only the Z component of the impulse is nonzero under integration over t and is given by $2[ue/b^2\nu]\int_0^{+\infty}(y^2 - 2)/(1 + y^2)^{5/2}dy$, where $y = ut/b$ in a direction (plus sign) away from the center of the nanoparticle. The net energy transferred, ΔE, to the electron of mass m due to the flowing dipoles can be estimated by integrating $\Delta\vec{p}^2/2m$ over the allowed range of b: $(\pi N/m)\int_{b_{\min}}^{b_{\max}}(\delta p)^2 bdb$. Here, N is the number of the flowing dipoles per unit area, the minimum of b is approximately the size of the dipole, and its maximum is the separation between the plates. The value of ΔE for large N can be larger than the surface work function which is typically less than the bulk value (for gold, 5.2 eV), thus creating a favorable situation for the ejection of the electron from the surface of the nanoparticle.

The ejected charges [11] would tend to stay in the vicinity of the oppositely charged nanoparticle. However, these would be affected by the convection velocity, u in the ξ direction. Let us assume that the perturbation is small so that at a given instant a number of charges are present around the nanoparticle that will screen the attraction [11] between the nanoparticle and the streaming charge, given by $V_{\text{screen}} = -Ze^2\exp^{-\mathcal{K}r}/\in r$, where $r = \sqrt{(\xi^2 + z^2)}$, ε being the dielectric constant of the medium. Ze the net charge induced on the nanoparticle and $\mathcal{K}$ being the inverse Debye screening length [9] due to countercharges around the nanoparticle [12]. This force will compete with the streaming velocity so far as $\mathcal{K}$ is not too large, the dominant competing forces being indicated schematically in Fig. 2(a). Note that the charged carriers will be subject to additional systematic forces: (1) The force of interaction with the flowing dipole with velocity u, given by $-e\vec{E}$ with components, $E_z = [3n_z(n_z\mu) - \mu]/[(Z + b)^2 + (\xi + ut)^2]^{3/2}$ and $E_\xi = [3n_\xi(n_\xi\mu) - \mu]/[(z + b)^2 + (\xi + ut)^2]^{3/2}$, where the unit vector components are $n_Z = (Z + b)/[(z + b)^2 + (\xi + ut)^2]^{3/2}$ and $n_\xi = (\xi + ut)/[(Z + b)^2 + (\xi + ut)^2]^{3/2}$. (2) A steeply repulsive interaction to ensure that the ejected charge carrier cannot penetrate the core of the nanoparticle after ejection: $V_{\text{rep}} = V_{\text{rep}}^0/r^{12}$, V_{rep}^0 being the magnitude of the repulsion at the unit separation. Further, the large saturation time scale involved in the experiments indicates a strong damping of the motion of the charge carriers in the complicated network of the nanoparticles. The thermally averaged overdamped [10] velocity components will be given by $\frac{\partial}{\partial t} \times \langle\xi\rangle = -\langle\frac{1}{\Gamma}[-eE_\xi + \frac{\partial(V_{\text{screen}} + V_{\text{rep}})}{\partial\xi}]\rangle + u$ and $\frac{\partial}{\partial t}\langle z\rangle = -\langle\frac{1}{\Gamma} \times [-eE_z + \frac{\partial(V_{\text{screen}} + V_{\text{rep}})}{\partial z}]\rangle$. Γ is the phenomenological damping coefficient [13]. We expand the force components about the mean $\langle\xi\rangle, \langle z\rangle$ and retain only the first term in the expansion as in mean field approximations. The resulting set of equations are solved numerically to obtain $\langle\xi\rangle, \langle z\rangle$ with the initial conditions that $\langle\xi\rangle = d/2$, $\langle z\rangle = d$ at $t = 0$ and obtain $\nu_S^* = \sqrt{[\frac{d}{dt}\langle\xi\rangle]^2 + [\frac{d}{dt}\langle z\rangle]^2}$, d being the diameter of the nanoparticle. The velocity at the surface $z = 0$, ν_S^*, is proportional to the flux of the charge carriers

at the surface which measures the charge accumulation at the surface and hence the ϕ_s.

We choose the length unit of $l = 10^{-7}$ cm, a typical nanoscale, the time unit of $\gamma = 10^{-6}$ s, a typical diffusion time of a molecule in the still analyte liquid and energy unit, $\varepsilon = e^2/l$. Figure 2(b) shows an increase in $\nu_S^* = \nu_S \tau/l$ as a function of $u^* = u\tau/l$ for a given $\gamma^* = \gamma\varepsilon/l^2\tau^{-1}$ in the $\mathcal{K}^* = \mathcal{K}/l \to 0$ limit, qualitatively similar as in the experiments. For large u, the charge carrier is driven far from the nanoparticle so that the systematic part of the velocity becomes less dominant, giving rise to linear increase in ν_S^* with u^*, qualitatively similar to the experimental observations in the large flow rate regime. Figure 2(c) shows that ν_S^* decreases with $\mu^* = e\mu\tau/l\gamma$, as in the experiments. As increasing γ^* results in the decrease in the systematic part of the velocity, we observe that ν_S^* decreases with γ^*. Since the damping is purely phenomenological, this trend is difficult to compare with the experimental observations. Finally, the addition of salt results in better screening and an increase in $\mathcal{K}$. For a finite but small $\mathcal{K}^*$, we find that ν_S^* decreases with increasing $\mathcal{K}^*$ due to the enhanced screening, similar in trend found in the experiments on adding salts.

In conclusion, we show here the possibility of devising flow sensors by nanoparticles. We shall call the effect as the transverse electrokinetic effect to emphasize its difference from the conventional electrokinetic effect where the streaming potential develops parallel to the flow [2]. The charges are knocked out of the nanoparticle surface by the Coulomb collision of the flowing dipoles which form a layer of countercharges around the charged nanoparticle. However, the layer of countercharges is destabilized as the charges are subject to the streaming flow in the presence of an attractive screened Coulomb force field due to the charged nanoparticle. The transverse voltage is generated by the damped motion of the carrier charges via the competition of these two force fields. The large voltage signal from this device, in contrast to that obtained from other methods [1,2], and quick adaptability to smaller dimensions with simple chemistry suggest potential applications in diverse fields including nanofluidics. We envisage measurement and control devices incorporated in flows through long channels, especially in biological context, wherein electrical connections from either end of the channel may be practically impossible.

The nanoparticle research program of T. P. is supported by the Department of Science and Technology. C. S. thanks the Council of Scientific and Industrial Research (CSIR) for additional support.

*Electronic address: pradeep@iitm.ac.in
†Electronic address: jaydeb@bose.res.in

[1] S. Ghosh, A. K. Sood, and N. Kumar, Science **299**, 1042 (2003).
[2] J. Yang, F. Lu, L. W. Kostiuk, and D. Y. Kwok, J. Micromech. Microeng. **13**, 963 (2003).
[3] P. Kral and M. Shapiro, Phys. Rev. Lett. **86**, 131 (2001).
[4] A. K. Sood and S. Ghosh, Phys. Rev. Lett. **93**, 86 601 (2004).
[5] J. Turkevich, P. L. Stevenson, and J. Hiller, Discuss. Faraday Soc. **11**, 55 (1951).
[6] The potential difference generated was around 3 mV for a single nanoparticle layer, which increased with an increase in the number of layers (≤ 5 layers). However, for a number of layers ≥ 5, nanoparticle layers were not stable in the flow for extended periods. Hence, we work with three layers to ensure stability and good voltage response under flow.
[7] N. Sandhyarani and T. Pradeep, Int. Rev. Phys. Chem. **22**, 221 (2003).
[8] Our data are inadequate to bring out the dependence of transverse potential on the flow at low flow rates. The experimental setup, consisting of the cylindrical housing with the flow device suspended, made it difficult to stabilize lower flow rates.
[9] J. D. Jackson, *Classical Electrodynamics* (John Wiley & Sons, New York, 1999), 3rd ed.
[10] The impulse acting on the dipole is $\sim(m/M)$, m and M the masses of electron and dipole, respectively, and is small for $m \ll M$. Similarly, angular displacement of the dipole during the collision, $\sim$(Coulomb energy)/(moment of inertia), is also small, considering the large moment of inertia of the flowing molecules and the distances involved.
[11] We assume that the carrier has an effective charge $-e$ without elucidating its detailed nature. The carrier of charge in this system need not be ejected electrons themselves; rather it can be some charged complex, formed via solvation in the polar fluid [B. Bagchi and R. Biswas, Adv. Chem. Phys. **109**, 207 (1999)].
[12] The equipotential nature of the metal surface has been ignored in this simple qualitative study. This can be incorporated by the standard method of electrostatics [9].
[13] P. M. Chaikin and T. C. Lubenski, *Principles of Condensed Matter Physics* (Cambridge University Press, Cambridge, England, 1995).